



Evolution of fuel plate parameters during deformation in rolling



M. Durazzo ^{a,*}, E. Vieira ^a, E.F. Urano de Carvalho ^a, H.G. Riella ^{a,b}

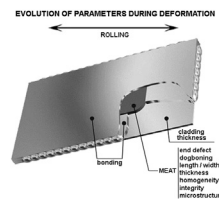
^a Nuclear and Energy Research Institute – IPEN/CNEN-SP, São Paulo, Brazil

^b Chemical Engineering Department, Santa Catarina Federal University, Florianópolis, Brazil

HIGHLIGHTS

- Evolution of defects when manufacturing dispersion fuel plates.
- Aspects of dispersion fuel plates fabrication.
- What happen during the manufacturing of dispersion fuel plates?
- Clarifying the deformation of fuel plates by rolling.

GRAPHICAL ABSTRACT



ARTICLE INFO

Article history:

Received 17 February 2017

Received in revised form

12 April 2017

Accepted 13 April 2017

Available online 14 April 2017

Keywords:

Fuel plate
Nuclear fuel
Dispersion fuel
Research reactors
Fuel fabrication
Silicide fuel

ABSTRACT

The Nuclear and Energy Research Institute – IPEN/CNEN-SP routinely produces the nuclear fuel necessary for operating its research reactor, IEA-R1. This fuel consists of fuel plates containing U_3Si_2 -Al composites as the meat, which are fabricated by rolling. The rolling process currently deployed was developed based on information obtained from literature, which was used as a premise for defining the current manufacturing procedures, according to a methodology with an essentially empirical character. Despite the current rolling process being perfectly stable and highly reproducible, it is not well characterized and is therefore not fully known. The objective of this work is to characterize the rolling process for producing dispersion fuel plates. Results regarding the evolution of the main parameters of technological interest, after each rolling pass, are presented. Some defects that originated along the fuel plate deformation during the rolling process were characterized and discussed. The fabrication procedures for manufacturing the fuel plates are also presented.

© 2017 Elsevier B.V. All rights reserved.

1. Introduction

Research reactors are used primarily for producing radioisotopes and materials testing. The IEA-R1 research reactor of IPEN/CNEN/SP is used for primary radioisotopes production, mainly ^{131}I . The fuel element for the IEA-R1 reactor is formed by assembling a series of spaced fuel plates, allowing the passage of a water flow that serves as coolant and moderator. The fuel element is composed of 18 flat and parallel fuel plates.

Since 1988, IPEN has been manufacturing fuel for the IEA-R1 reactor. The picture-frame technique is used [1,2]. The fuel currently produced adopts the U_3Si_2 -Al dispersion with uranium concentration of 3.0 gU/cm^3 [3]. The rolling procedures currently implemented have been developed based on literature information [4–6], which were used as premises for defining the current manufacturing procedures, according to an essentially empirical methodology. For this reason, even though the current rolling process is perfectly stable and highly reproductive, it is not well characterized and is therefore not fully understood.

The knowledge of the rolling process adopted for fabricating fuel plates is important to understand and to correct possible deviations that might occur in the manufacturing process. Furthermore, a deeper understanding of this process allows for adjusting it

* Corresponding author. Av. Prof. Lineu Prestes, 2242, Cidade Universitária, CEP 05508-000, São Paulo, SP, Brazil.

E-mail address: mdurazzo@ipen.br (M. Durazzo).

quickly to new specifications, in the case of manufacturing fuels for use in other research reactors. This is especially important since a new research reactor is planned to be built in Brazil [7–9] and IPEN will have the incumbency of providing the fuel for the new reactor research.

The objective of this work is to characterize the rolling process currently adopted by IPEN, specifically regarding the evolution of dimensional parameters of the fuel plate as a function of its deformation in the rolling process. The parameters studied were length, width and thickness of the fuel meat, thickness of the cladding, dog-boning evolution, bonding evolution, and microstructure of the meat.

2. Experimental

2.1. Description of fuel plate manufacturing

The method for manufacturing fuel plates by a hot and cold rolling sequence is well-developed, and has been extensively used for the production of fuel elements for many research reactors around the world. The fuel element is an assembled set of fuel plates. It consists of regularly spaced parallel plates forming a fuel assembly. The fuel plates have a meat containing the fissile material, which is entirely clad with aluminum. They are manufactured by adopting the traditional assembling technique of a fuel meat (or “briquette”) inserted in an aluminum frame and clad by aluminum plates, which are bonded with subsequent rolling.

Powder metallurgy techniques are used in the manufacture of the briquette, which uses U_3Si_2 as the uranium fissile composite. The briquette is made with powdered fissile material and pure aluminum powder, which is the structural matrix material of the briquette. Fig. 1 presents scanning electron micrographs showing the typical appearance of U_3Si_2 (A) and aluminum (B) particles. After rolling, the briquette composes the meat of the fuel plate, which is perfectly isolated from the external environment, protected by the aluminum cladding. The briquette is a rectangular parallelepiped with rounded corners. The powders for each individual briquette are separately weighed and combined for blending. For pressing the briquettes, a pressing pressure of about 5 ton/cm² is used.

The picture-frame technique [1,2] is used to produce the fuel plates, where the briquettes are processed with mechanical working. An assembly is used, which consists of a frame, the fuel meat (briquette) and two cover plates, as illustrated in Fig. 2. The assembly is converted into plates to provide the required dimensions and complete sealing of the fuel. The frame provides both lateral support and material for the cladding. The briquette and frame are bonded to the covers by hot bonding during a hot-rolling processing. The material used as frame and covers is 6061 aluminum.

The final dimensions specified for the fuel plates are 625 mm long by 71 mm wide by 1.52 mm thick. The dimensions of the fuel meat are 600 mm long by 65 mm wide by 0.76 mm thick. The thickness of the frame plate is 4.2 mm and the thickness of the cover plates is 2.5 mm. The width and length of the frame and cover

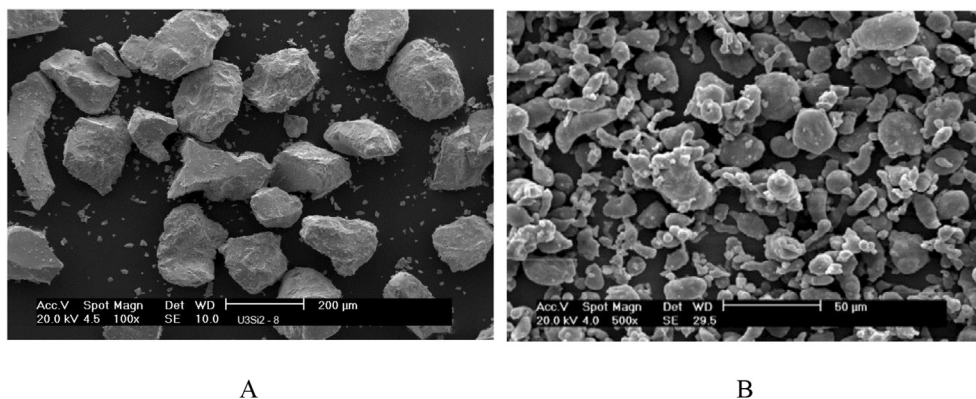


Fig. 1. Typical morphology of U_3Si_2 (A) and Al (B) powders (secondary electrons).

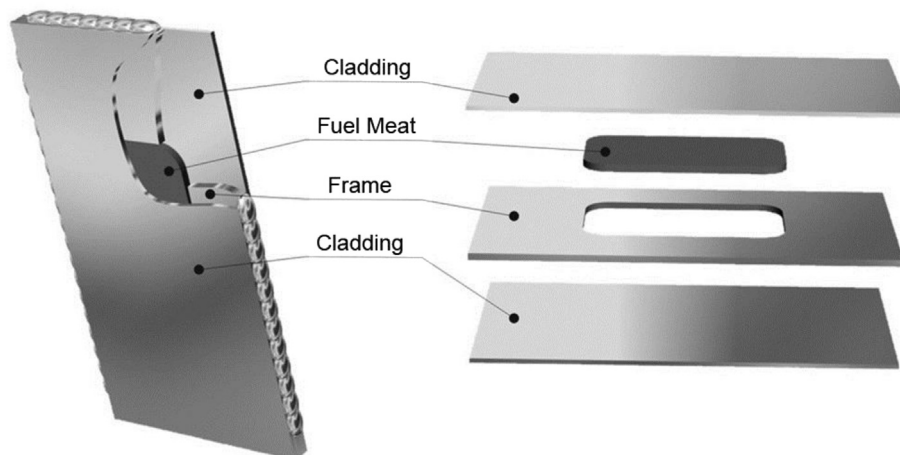


Fig. 2. Diagram illustrating the assembling of the set meat-frame-covers.

Table 1
Hot-rolling schedule.

| Pass | Reduction (%) | Gage (mm) | Heating Time (min) |
|------|---------------|-----------|--------------------------|
| 0 | 0 | 9.20 | preheating (60 min) |
| 1 | 25 | 6.93 | 15 |
| 2 | 25 | 5.20 | 15 |
| 3 | 15 | 4.42 | 15 |
| 4 | 15 | 3.76 | 15 |
| 5 | 15 | 3.20 | 15 |
| 6 | 15 | 2.72 | 15 |
| 7 | 15 | 2.31 | 15 |
| 8 | 13 | 2.01 | 15 |
| 9 | 13 | 1.75 | blistering test (60 min) |

plates should ensure a sufficient quantity of material around the briquette so that the structural function of the frame is fulfilled. The dimensions used were 200 mm long by 120 mm wide.

Picture frames and cover plates are identified with a number printed on the outside of each top cover which relates the assembly with the lot number and briquette number. An X marks the position of the assembly to orientate the rolling operation. It is important to have a reference when making a fuel plate and this X identifies the reference edge and reference end of the fuel plate. To achieve a good bonding quality, the frames and covers are wiped with acetone and further etched using a tank with 10 wt% sodium hydroxide solution and 40% nitric acid.

For assembling, a bottom cover plate is laid out on a table top, and the briquette is placed over the cover plate. Tongs are used to handle both frames and briquettes. Frames are placed in a rack and

preheated in a furnace for 35 min at 450 °C. The heated frame is then quickly placed on top of the briquette, which is seated in the expanded cavity of the frame. The top cover plate is placed and held firmly on the top of the assembled frame. The briquette is kept in position until the frame has cooled sufficiently to lock the briquette in place. After the frame has cooled, the top cover is removed and the briquette is checked for seating. The top cover is replaced and each assembly, in turn, is carefully aligned and TIG welded. This procedure ensures that the clearances between the briquette and the cavity of the frame are as small as possible. Approximately 10 mm from each corner of the set is left unwelded to permit escape of any entrapped air.

The assemblies are hot-rolled to be converted into plates and to provide a bond between the cover plates and the frames and briquettes. The assemblies are preheated for 1 h in an electric furnace with a hot-air circulation blower. The hot-rolling temperature is 450 °C. The assemblies are reheated for 15 min between rolling passes. The hot-rolling schedule is presented in Table 1. The thickness of the hot-rolled plate is measured with a tungsten-carbide-tipped hot micrometer after each pass.

To control the end defects and cambering, the assemblies are rotated about their longitudinal and transverse axis between passes. The main end defects are dog-boning and “diffuse zone”. Inevitably, the rolling process leaves the ends of the meat thicker than the middle. The longitudinal cross section of a fuel meat with thickened ends resembles a bone, hence the name (see Fig. 3). The “diffuse zone” refers to the defects known as “fish-tail” (see Fig. 3) and also the distortion of the geometry of the end of the fuel meat caused by cambering. Fig. 4 shows a schematic drawing illustrating the cambering defect and the consequent geometry distortion of the end of a fuel meat.

The end defects and cambering are minimized by applying an appropriate rotation scheme during the rolling of the fuel plates. Usually, the assembled sets have an identification number and a X mark on the upper cover plate. This type of identification allows the operator to control the scheme of the assembly rotation during rolling, from the first to the last rolling pass. In the first pass of rolling the X mark is in the upper surface of the assembly, on the edge opposite the edge entering the rolling rolls. For the second pass, the assembly is rotated 180° in its longitudinal direction and also 180° in its transverse direction. These rotations are performed simultaneously when the assembly comes out of the rolling mill in the first pass. After the rotations, the X mark for the second pass is on the bottom surface of the assembly, at the edge that will enter the rolls. Fig. 5 shows the rotation scheme.

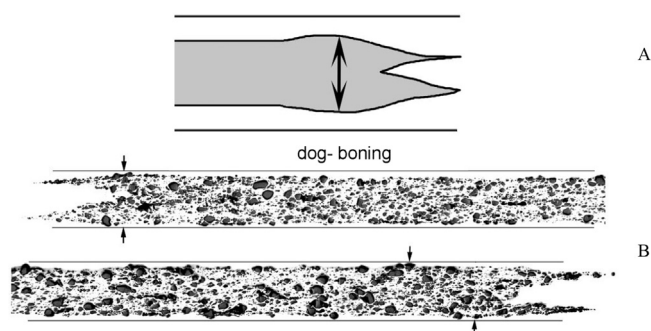


Fig. 3. End defects known as “dog-boning” and “fish tail”. A-schematic, B- real.

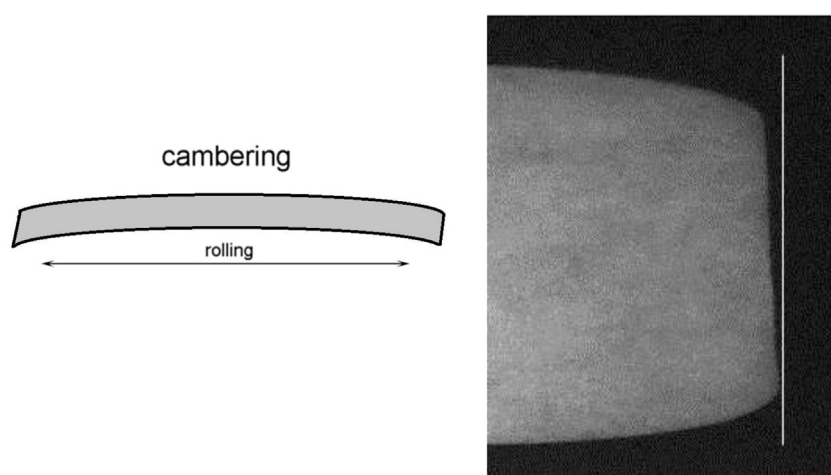


Fig. 4. Illustration of the cambering defect.

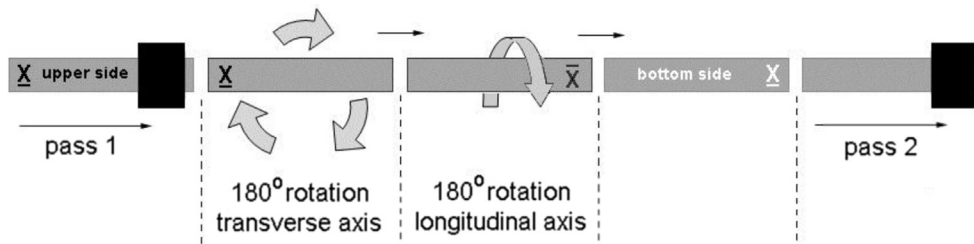


Fig. 5. Illustration of the rotation scheme in the rolling operation.

Table 2
Cold-rolling schedule.

| Pass | Reduction (%) | Gage (mm) | Heating Time (min) |
|-------|---------------|-----------|--------------------|
| 0 | 0 | 1.75 | from hot-rolling |
| 10 | 7 | 1.63 | no heating |
| 11 | 6–7 | 1.53–1.51 | no heating |
| final | 0 | 1.53–1.51 | final adjustment |

For the third pass, the same procedure is applied, turning the assembly 180° in its longitudinal direction and 180° in its transverse direction, returning to the entering position in the first pass. In the fourth pass, the entering position is the same as the second, and so on. Passes with odd numbers have the same entering position as the first pass and passes with even numbers have the same entering position as the second pass.

After the last rolling pass, the fuel plates are furnace annealed at 450°C for 1 h at temperature. The plates are removed from the furnace, cooled, and inspected for blisters. This blister test must be done to inspect the fuel plate for possible bonding imperfections between frames, covers and fuel meat. Blisters are generated in non-bonding sites, the sites being caused by contamination. Lint from gloves, backstreaming of vacuum pump oil, fumes generated in the hot-rolling furnace, too much oil on the rolls during the first hot-rolling pass, and organic contamination in nitric acid all can cause blisters.

The cold-rolling operation is done by using a high precision mill and two rolling passes, as presented in Table 2. The accuracy of the mill is about 0.02 mm.

After cold-rolling, the next step in the manufacture is to x-ray the fuel plate to lay out the core in preparation for bringing the fuel plate to its final specified size. Before the final shearing operation, a preliminary shearing is done to facilitate the posterior flattening and fuel meat location. The fuel meat is visually located by the operator and the preliminary shearing is done with a precision guillotine. After the preliminary shearing the fuel plates are

flattened using a roller leveler. For the final shearing operation, the fuel meat is precisely located and reference lines are drawn in the pre-cut plate to locate the edges and corners of the fuel plate in its final dimension.

After cold-rolling, the bond integrity is also inspected by the bend test. Excess cladding is trimmed of the fuel plate in the final shearing operation. Leftover trimmings of the aluminum cladding, directly adjacent to the final plate, are subjected to bend tests as a means of evaluating bond quality. Bend test samples are taken from all four sides of each plate. Each sample is clamped in a test fixture and bent around a mandrel 90° in one direction, returned to 0° , bent 90° in the opposite direction, and returned to 0° . The edges of the bend test sample which were adjacent to the final plate are then visually examined for delamination. Any strip showing delamination of the cladding layers is determined to be unbonded and the associated plate is rejected. Fig. 6 shows samples after the bending test.

The final dimensions of the fuel plate are determined by measuring its final length, width and thickness. The length is measured in 3 positions by using a 0.02 mm precision caliper and the width is measured in 7 positions by using a 0.01 mm precision micrometer. The fuel plates are inspected for thickness to the nearest 0.01 mm at 21 positions per plate with a deep throat micrometer with nonrotating spindles having chamfered edges. The fuel meat outline is inspected by an x-ray scanner and the fuel meat length and width are measured directly in the x-ray scanner. The maximum fuel meat width and length are determined with precision of 0.01 mm. The diffuse zone at the end of the fuel meat (“fish-tail” plus geometry distortion due cambering) is considered as meat length. Usually the width of the zone diffuse is at most 2 mm. The cambering is considered as meat width. Also, the fuel meat centering is inspected by determining the widths of the cladding at the edges and ends directly on the x-ray scanner screen. The minimum widths are determined and the differences between widths are calculated to ensure that the fuel meat is centered. The cladding and meat thicknesses are measured by means of

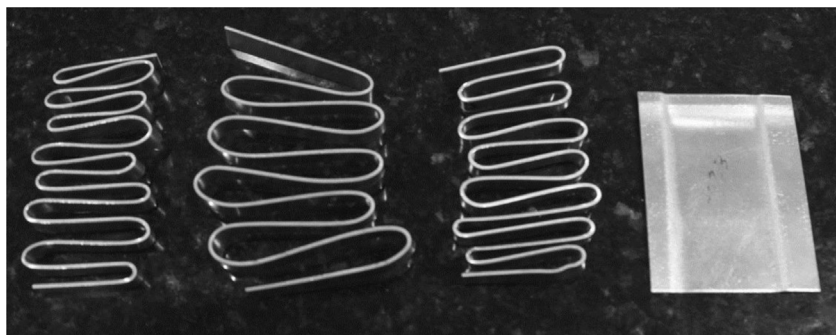


Fig. 6. Bend test examples. Left - length side. Right - width side.

metallography. The homogeneity in the uranium distribution inside the fuel meat and the fuel meat integrity are inspected by x-ray.

2.2. Parameters studied

The fuel plate fabrication process is performed with nine hot-rolling passes and two cold-rolling passes. Thus, 12 briquettes with U_3Si_2 -Al dispersions were produced according to the current specifications of the fuel fabricated at IPEN for use in the IEA-R1 research reactor, with a uranium density of 3.0 gU/cm^3 . All produced briquettes meet the specification and were manufactured strictly according to well-established procedures. All briquettes were assembled and rolled as specified for the fuel plate production, according the procedures explained before. A plate was removed after each rolling pass, generating a sample at each stage of the deformation of the fuel assembly. In this way, samples taken after each rolling pass represents the status of a fuel plate in that stage of the rolling process. A briquette was studied just after pressing, i.e. without undergoing the rolling process. This briquette provided microstructural information of the initial fuel meat.

The samples were analyzed for the most important aspects of the U_3Si_2 -Al fuel meat, namely:

- 1 end defects geometry;
- 2 thickening of the meat at its end, which is a defect known as "dogboning";
- 3 fuel meat integrity;
- 4 bonding;
- 5 homogeneity of uranium distribution;
- 6 fuel meat microstructure;
- 7 length of the fuel meat;
- 8 width of the fuel meat;
- 9 cladding thickness in the meat region;
- 10 thickness of the fuel meat;

These parameters were studied with the aid of x-rays and traditional measurement instruments, such as rulers and calipers, as well as traditional metallography techniques and image analysis for thicknesses measurements.

Metallography is widely used by manufacturers for the inspection of the thickness of claddings and fuel meats of fuel plates [10,11]. The cladding thickness of the fuel plate is of great importance for the function of the fuel plate in the fuel element; therefore, it is strictly specified. After each rolling pass, the fuel plate was submitted to destructive cladding thickness measurements by cutting rectangular sections of about 10 mm width by 20 mm length at four positions. Two specimens were cut out from the end regions of the fuel meat (dog-bone region) and two specimens were cut out from the central region of the meat (one longitudinal, or in the rolling direction, and one transversal). The measurement was performed by taking the minimum values of the cladding in each specimen in selected positions where visually the cladding thickness is decreased. Metallography is also used to study the geometry of the end defects and the microstructural aspects of the fuel meat.

To take out the samples from the fuel plate for metallographic examination the meat was located through radiograph and the locations where the samples will be taken were marked. The samples were then removed from the fuel plate. First a "pre-cut" (or coarse cut) is performed on the four demarcated regions. This operation is accomplished using a manual guillotine. To make the final shearing accurate, a cutter with a diamond disc was used. The samples were properly identified and were embedded in acrylic resin. Once the samples were embedded, each sample was prepared according to the following steps:

- 1 Grinding with SiC 320 grit-paper;
- 2 Grinding with SiC 600 grit-paper;
- 3 Grinding with SiC 1200 grit-paper;
- 4 Polishing with $6 \mu\text{m}$ diamond paste;
- 5 Polishing with $3 \mu\text{m}$ diamond paste;
- 6 Final polishing with $0.02 \mu\text{m}$ colloidal silica slurry.

For each step, a grinding time of three minutes was used (70 rpm). For the steps of diamond polishing, a polishing time of 15 min was used (70 rpm). For the final polishing step, a polishing time of 5 min was used.

The homogeneity of uranium distribution and the fuel meat integrity were inspected by using an x-ray scanner. The images of the fuel meat were analyzed directly in the high-resolution scanner screen.

3. Results and discussion

3.1. Evolution of defects

The presence of some important defects in the fuel meats after rolling was studied. Structural defects such as cracks and fish tail were related to certain features of the set meat-frame-covers (Fig. 2). The uranium distribution homogeneity in the fuel meat was sensitive to the particle size distribution of the aluminum powder.

Special care should be taken with regard to the difference between the thickness of the briquette and the thickness of the frame plate. If the thickness of the briquette is lower than the thickness of the frame plate an irreparable defect will occur at the end of the fuel meat of the finished fuel plate, like a mark of chewing type (a depression that can lead to rupture of the cladding at the end of the fuel meat). On the other hand, if the thickness of the briquette is higher than the thickness of the frame plate, the briquette material will flow between the frame and the covers, resulting in an unacceptable increase in the end defect "fish tail", which is a lengthening of the end of the core, as illustrated in Fig. 3. It was found that the thickness of the briquette should be slightly greater than the frame thickness (0.1–0.2 mm) to avoid these defects.

A preferred deformation of the cladding during the rolling operation was observed. This is due to the higher resistance to deformation of the fuel meat caused by the presence of U_3Si_2 particles, which causes a greater lengthening in the claddings. This is also a cause for the typical end defect known as "fish-tail", illustrated in Fig. 3, which is due to the difference in strength between the meat and the claddings. For this reason, even if the thicknesses of the briquette and frame plate are the same, the "fish tail" defect will inevitably occur to a certain degree. Note that the core ends protrude into the frame/cladding interface by the forced deformation of the claddings, while the central meat region does not follow the deformation. In other words, the flow of meat and claddings during the deformation in rolling is different due to the differences between the mechanical properties of these materials. The free aluminum of the claddings tends to flow more easily and the reduction in thickness and lengthening are higher. The top and bottom surfaces of the meat, which is in direct contact with the claddings, follow the flow of metal elongating more than its central region. This situation causes the "fish-tail" defect at the ends of the core, as already illustrated. Fig. 7 shows the evolution of this type of end defect during rolling. The terms "entrance" and "exit" shown in the figure refer to the actual position of the fuel plate on the rolling pass in question, disregarding the rotation scheme.

Note that this type of defect occurs already during the first hot-rolling pass, both at the entrance and exit of the rolls. In the sample related to the first pass, beyond the fish-tail, an empty region is

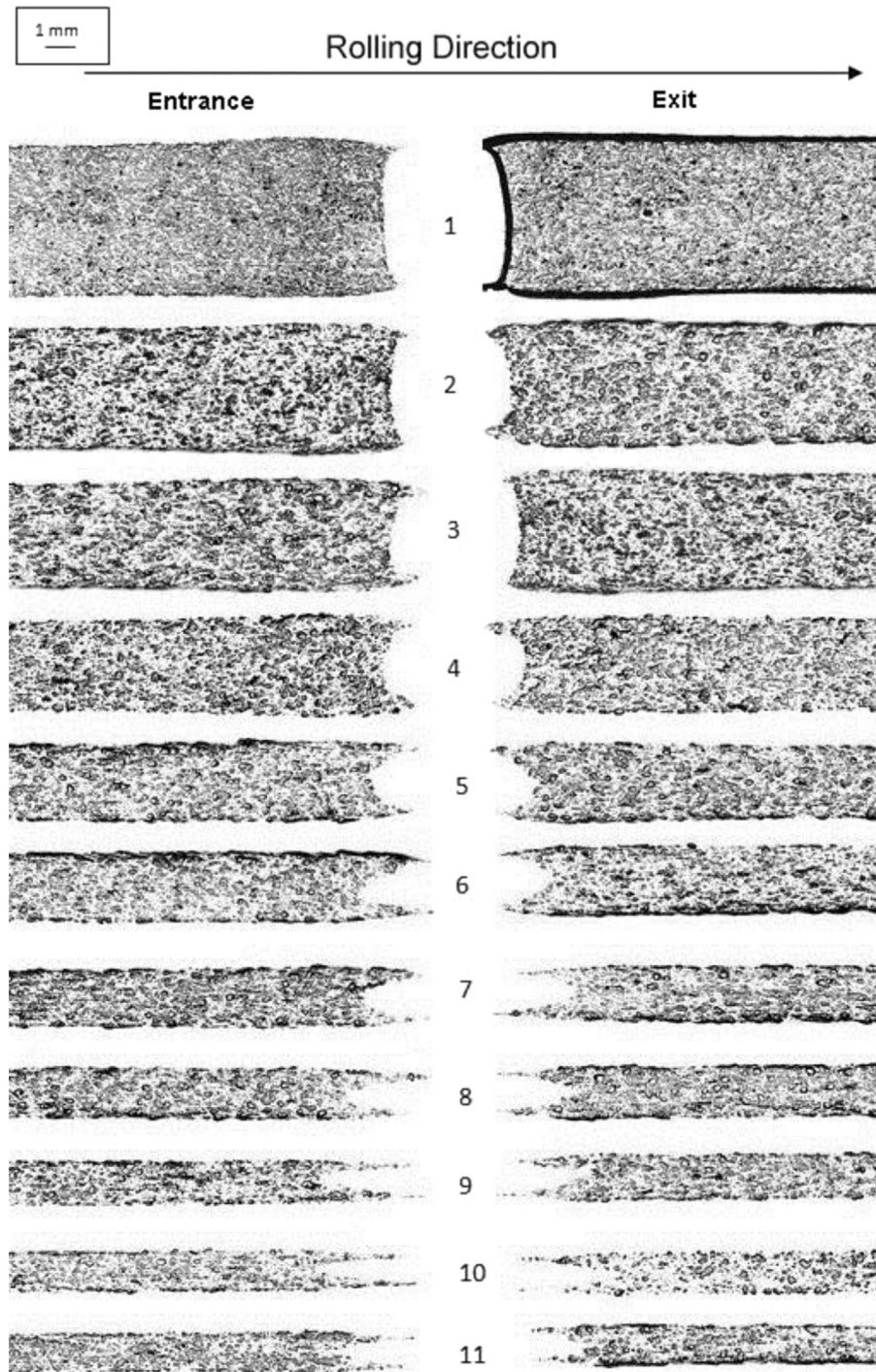


Fig. 7. Evolution of the “fish-tail” end defect during rolling a fuel plate.

observed at the exit side, which suggests that most of the voids caused by the adjustments of the picture-frame components concentrate on the end of the meat coming out of the mill. In the first pass, the geometry of the defect is apparently symmetric.

In the second rolling pass, a void at the exit end of the fuel plate can still be observed. Furthermore, it can be noticed that the fish-tail is more pronounced at the exit side in this rolling pass. In the third pass is interesting to note that at the entrance, which refers to the output of the previous pass, the frame appears to “hold” the central region of the meat, defining more

sharply the upper and lower extremities of the fish-tail. In this pass the void region observable in previous passes is no more observable, which indicates an already good level of bonding in low magnification observation. From the fourth pass onwards there is a good symmetry between the entrance and exit sides of the fuel plate.

The other typical end defect is the “dog-boning”, which is the thickening of the meat at its ends in the longitudinal axis of the fuel plate. This phenomenon is common in cases of simultaneous rolling of components that have different mechanical properties. In the

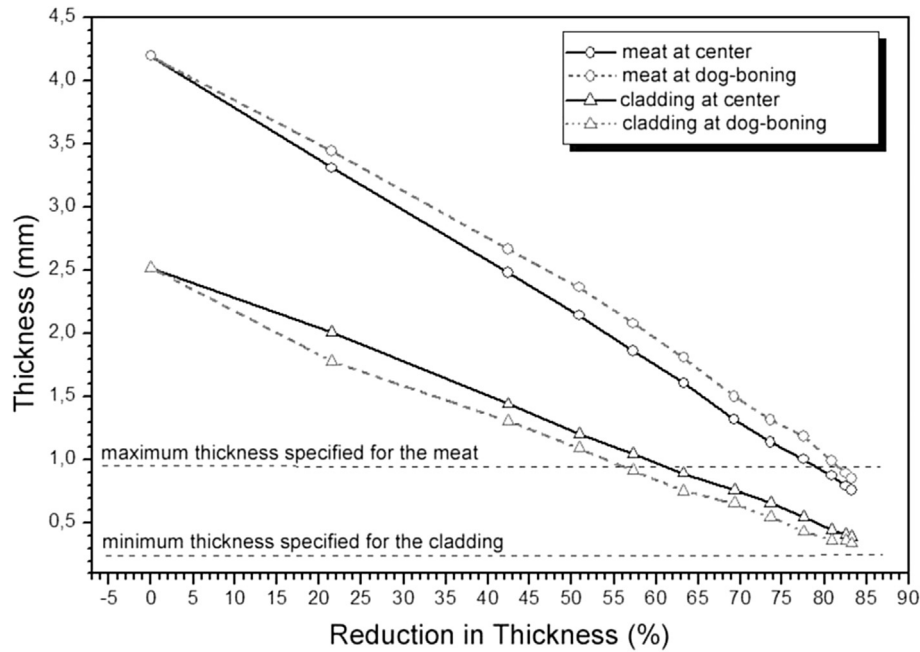


Fig. 8. Meat and cladding thicknesses at the dog-boning region as a function of deformation during rolling.

case of fuel plates, the meat is more resistant to deformation than the other aluminum components of the assembly (frame and claddings). Because of this, the rolling process produces thicker ends of the meat than its central region. This type of defect has two undesirable consequences: reduced cladding thickness at the end of the fuel meat and increased areal uranium density, which is the amount of uranium beneath a unit area of a plate surface. The latter may result in excessively high surface heat fluxes during irradiation and because for rejection of the plate. Therefore, the dog-boning must be considered in the fuel design to compensate for the decrease in the cladding thickness due to this inevitable defect. Fig. 3 illustrates this type of end defect.

Fig. 8 shows the evolution of the fuel meat and cladding thicknesses in the central and dog-boning zones of the fuel meat as a function of the fuel plate deformation. This figure shows that the thickening of the fuel meat (dog-boning) occurs mainly in the first hot-rolling pass, decreasing in the second pass and remaining almost constant until the ninth hot-rolling pass. The difference between the thickness of the meat at the center region and at the end region decreases slightly at the final hot-rolling pass and significantly in the cold-rolling passes.

After the last pass (in the finished fuel plate), the cladding thickness reaches a value slightly above the minimum specified

(250 μm). Apparently, at the end of rolling, particularly in the cold-rolling, the thickening of the core decreases, probably due to fragmentation of U_3Si_2 particles, which facilitates its deformation. The fragmentation of U_3Si_2 particles was experimentally observed in this work, as discussed in item 3.4 and illustrated in Fig. 15.

One of the functions of the frame is to provide lateral support for the briquette during the rolling procedure. It was observed that, if the briquette is smaller than the frame cavity and the fitting allows a gap between them, the edges of the briquette will crack during the first rolling passes. The result is the appearance of cracks on the edges of the fuel meat in the finished fuel plate, as illustrated in Fig. 9. The tendency for cracking the edges is more pronounced at the center of fuel meat, where the cambering is maximum.

This type of defect can be prevented by limiting the gap between the briquette and frame. This shrink fit was used in this work to assemble the briquettes into the frames, in such a manner that gaps are eliminated. The briquette width and length were designed to be identical to the frame cavity in order to obtain the interference fit between briquette and frame. No cracks were observed when interference fit was used. The maximum acceptable gap between the briquette and the frame cavity to avoid cracks is around 0.2 mm, but interference fit is recommended.

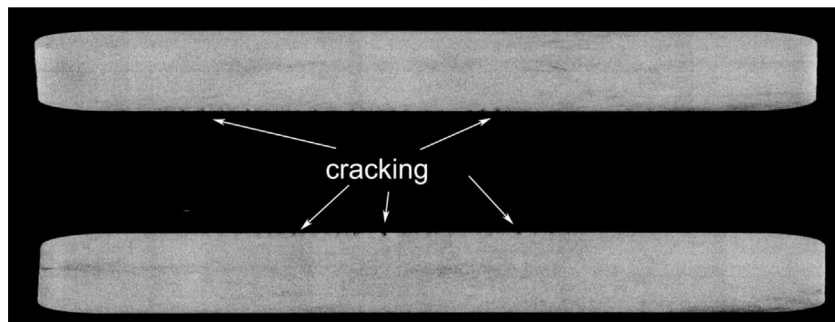


Fig. 9. Cracking caused by incorrect fit when assembling the briquette into the frame.

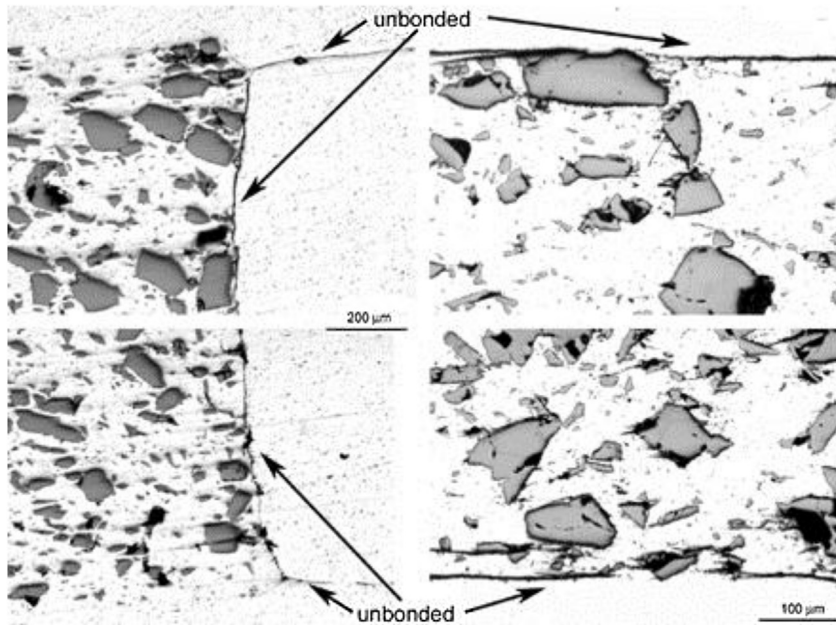


Fig. 10. Optical micrographs showing the absence of bonding at the center (right) and end (left) of the fuel meat (second hot-rolling pass).

3.2. Evolution of bonding

One of the main objectives of hot-rolling is to promote the bonding between the cover plates and the frames and the briquette. No bonding failure is allowed. As can be seen in Fig. 7, after the first hot-rolling pass no bonding is achieved. The bonding takes place continuously during the subsequent hot rolling passes. In the second hot-rolling pass the bonding between the meat and the cladding has not yet occurred in any region of the fuel meats. Fig. 10 presents micrographs of samples taken from the end and central regions of the fuel plate after the second hot-rolling pass, which show failure in the bonding between the meat and cladding and between the frame and claddings. The same situation is also observed after the third hot-rolling pass.

On the fourth hot-rolling pass a few bond failures can be observed. In the sample taken from the end of the meat, a tenuous line (shown in Fig. 11) indicating that the bonding between the core and the frame is not complete is still observed. In this region, no more failures between the frame and claddings are observed. In the sample taken from the center of the fuel plate, a nearly perfect bonding is evidenced, even if a single isolated region of localized bonding failure can be observed, as illustrated in the micrographs

shown in Fig. 11. These observations show that the bonding in the fourth hot-rolling pass is not yet perfect. In the fifth pass all regions of the meat are perfectly bonded although a defective bonding between the aluminum claddings and frame at the edges of the fuel plate still exists. In the sixth hot-rolling pass no longer bonding failures are detected.

The observations presented above are indications that the bonding occurs initially in the central region of the fuel plate, progressing to the extremities with continued rolling. It is noted that the gap between the components of the assembly is decreasing with the evolution of hot-rolling. At the center of the meat, the bonding is virtually completed in the third pass. At the lateral edge of the meat the bonding is practically completed in the fourth rolling pass. Fig. 12 shows a schematic diagram of how the bonding proceeds over the course of the rolling process. The bonding begins in the center of the fuel plate and progresses in all directions to the extremities.

3.3. Uranium homogeneity

One of the most important operations in the preparation of dispersion fuels is the uniform distribution of the fuel particles in

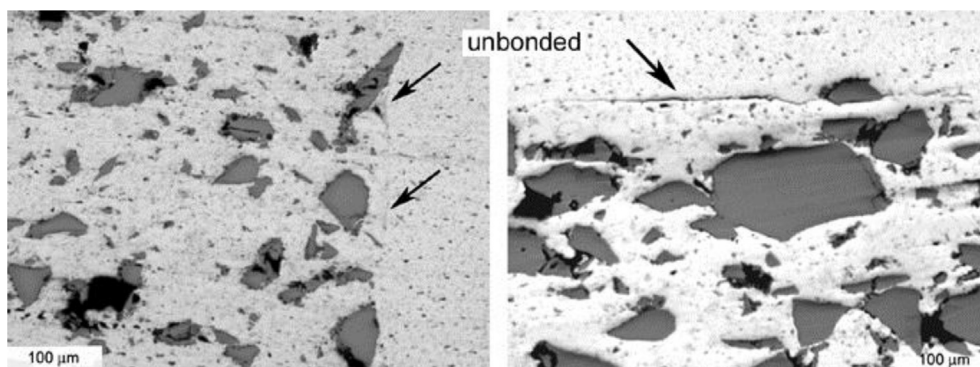


Fig. 11. Optical micrographs showing almost completed bonding at the center (right) and end (left) of the fuel meat (fourth hot-rolling pass).

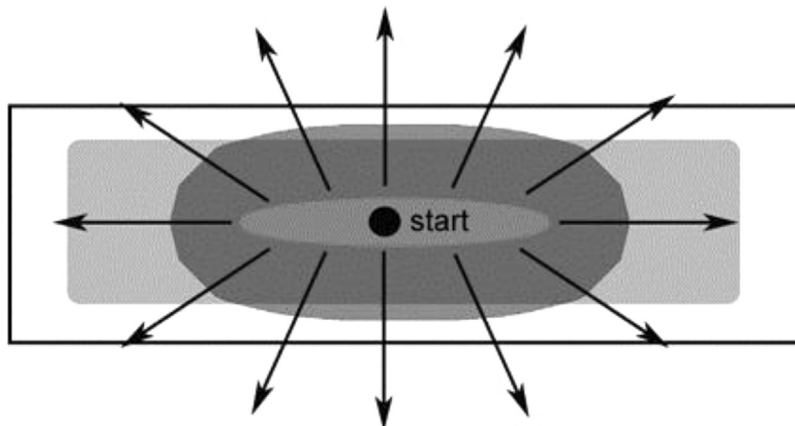


Fig. 12. Schematic illustration of the evolution of bonding with successive rolling passes.

the matrix material. If the distribution of the fuel particles is nonuniform, there will be localized regions in the fuel plate in which the fuel concentration is higher than average. This may cause a reduction in the irradiation stability and mechanical strength of the fuel plate in the course of operation. A good homogeneity in the uranium distribution inside the fuel meat is important from the standpoint of irradiation performance. Excessive fuel loading may cause unwarranted power peaking and “hot spots” during irradiation. Fuel plates which do not conform to fuel loading specifications are rejected. These loading specifications depend on the operation requirements of the fuel in a particular reactor. For low-performance reactors, areas with higher concentrations of fuel in the meat are not desirable but, unless very heavy, do not cause problems. In these cases, the commonly accepted technique for inspecting for such inhomogeneity has been a radiographic examination of the plates and visual comparison with a standard plate.

To provide a maximum control of the nominal uranium concentration, each briquette was weighed and blended individually. Furthermore, in order to avoid inhomogeneity, the Al powder was

dried and sieved before use. Sieving ensures deagglomeration of the Al powder.

Usually the particle size specification for the Al powder is less than $44\ \mu\text{m}$, and the fraction greater than $44\ \mu\text{m}$ is rejected. However, due to the large difference between the densities of the U_3Si_2 ($11.7\ \text{g}/\text{cm}^3$) and Al ($2.7\ \text{g}/\text{cm}^3$) powders, the mixture thereof has a strong tendency towards segregation during handling of loads for the feeding of the pressing die. It was found that the particle size of the Al powder strongly influences this tendency to segregation. The use of fine Al powder drastically reduces the segregation. A good average particle size (D_{50}) for the Al powder is around $10\ \mu\text{m}$. When the average particle size of the Al powder increases to $34\ \mu\text{m}$ (as shown in Fig. 13) the homogeneity of the fuel meat is impaired. Fig. 14 illustrated this effect. This figure compares the homogeneity of U_3Si_2 distribution in a fuel meat rolled from briquettes using Al powder with $D_{50} = 11\ \mu\text{m}$ (Fig. 14A) and $D_{50} = 34\ \mu\text{m}$ (Fig. 14B). Special care must be taken to ensure deagglomeration of the aluminum powder, otherwise defects caused by aluminum agglomerates as shown in Fig. 14C will arise in the form of elliptical marks on the

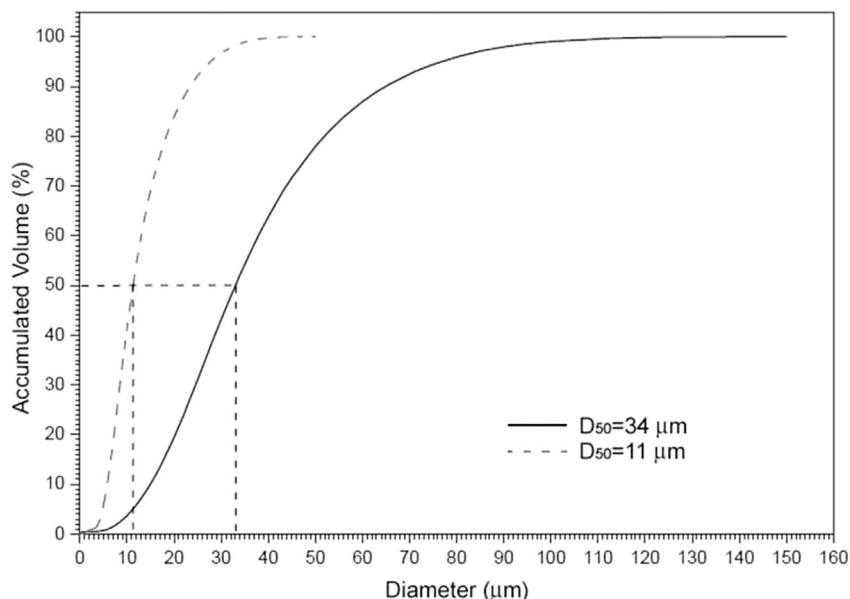


Fig. 13. Typical particle size distribution of Al powder used as matrix.

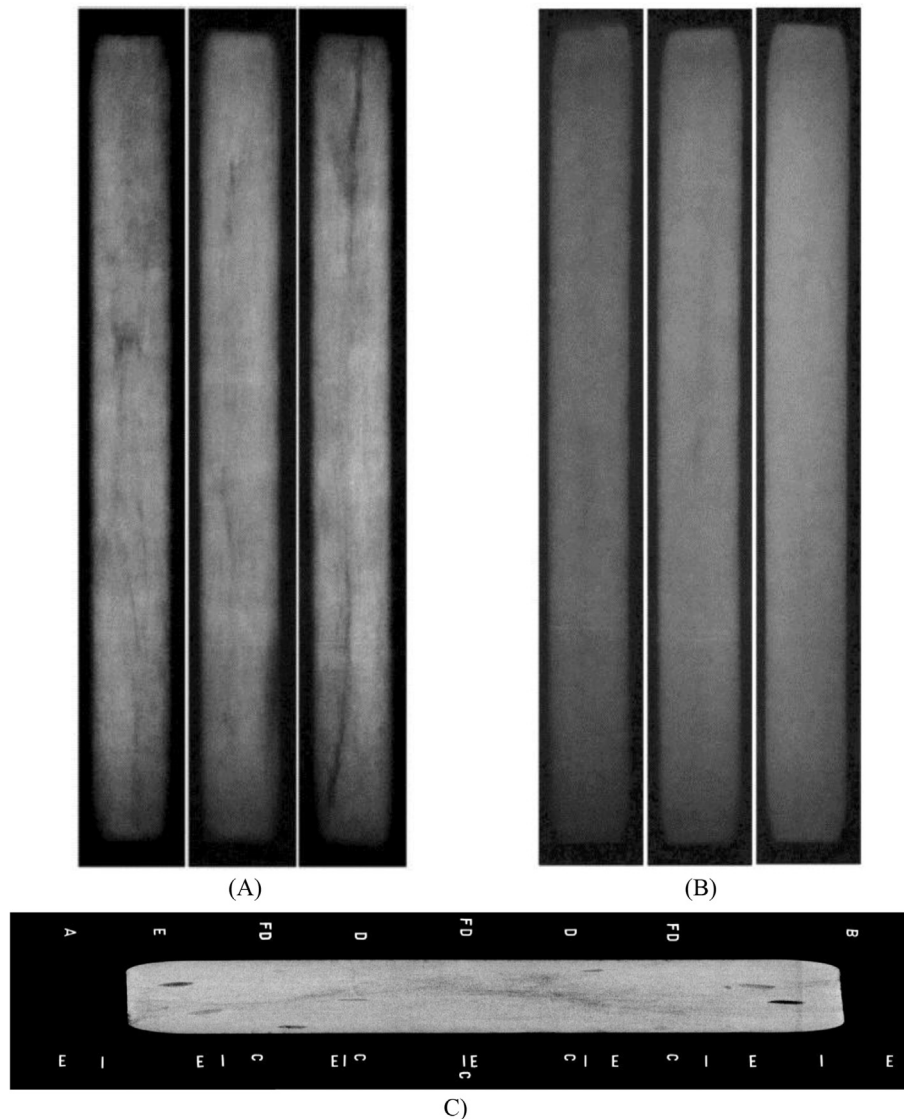


Fig. 14. Radiographs showing the effect of particle size of the Al powder on the uranium homogeneity in fuel meats. A – $D_{50} = 34 \mu\text{m}$, B – $D_{50} = 11 \mu\text{m}$, C – presence of aluminum agglomerates.

X-ray image. This can be easily avoided with a simple previous sieving of the aluminum powder.

The studies and results presented in this work were obtained from fuel plates whose cores had a good homogeneity in the uranium distribution, using aluminum with $D_{50} = 11 \mu\text{m}$.

3.4. Microstructure of the U_3Si_2 -Al dispersion

Porosity remaining after fabrication of dispersion fuel meat provides space to accommodate the initial swelling of the fuel particles under irradiation. The amount of as-fabricated porosity is related to particle fragmentation. The U_3Si_2 fragile particles fragment and it becomes more difficult for the aluminum matrix to flow completely around all fuel particles, especially those in contact with one another [12].

Low residual porosity is observed in the starting briquette and the U_3Si_2 particles remain almost intact. Small cracks can be seen in the particles and low porosity is evidenced (Fig. 15A). In the first rolling pass, the starting of U_3Si_2 particle fragmentation is observed without pronounced separation of the fragments (Fig. 15B).

Porosity starts to be formed due to fragmentation. Continuing hot-rolling, the porosity seems not to increase too much, but the amount of fine U_3Si_2 particles increases, showing fragmentation in the third pass (Fig. 15C). This situation remains until the end of hot-rolling, as shown in the microstructure presented in Fig. 15D for the ninth pass. In cold rolling, the fragmentation of U_3Si_2 particles is more pronounced. The maximum particle size decreases noticeably. The residual porosity also appears to increase slightly. The micrographs of Fig. 15E and F shows the microstructure of the meat for the two cold-rolling passes, the tenth and the eleventh pass, respectively.

Apparently, in the first hot-rolling pass, an initial U_3Si_2 fragmentation occurs. The fragments are separated leaving voids, but residual porosity does not appear to increase during hot-rolling after this initial void formation. Apparently the residual porosity of the fuel meat reaches equilibrium and remains unchanged throughout the hot-rolling. In cold-rolling, U_3Si_2 particles are fragmented, resulting in increased residual porosity. Some stringering (not much severe) can also be observed in the microstructure of the cold-rolled meats. The stringering is the fragmentation of

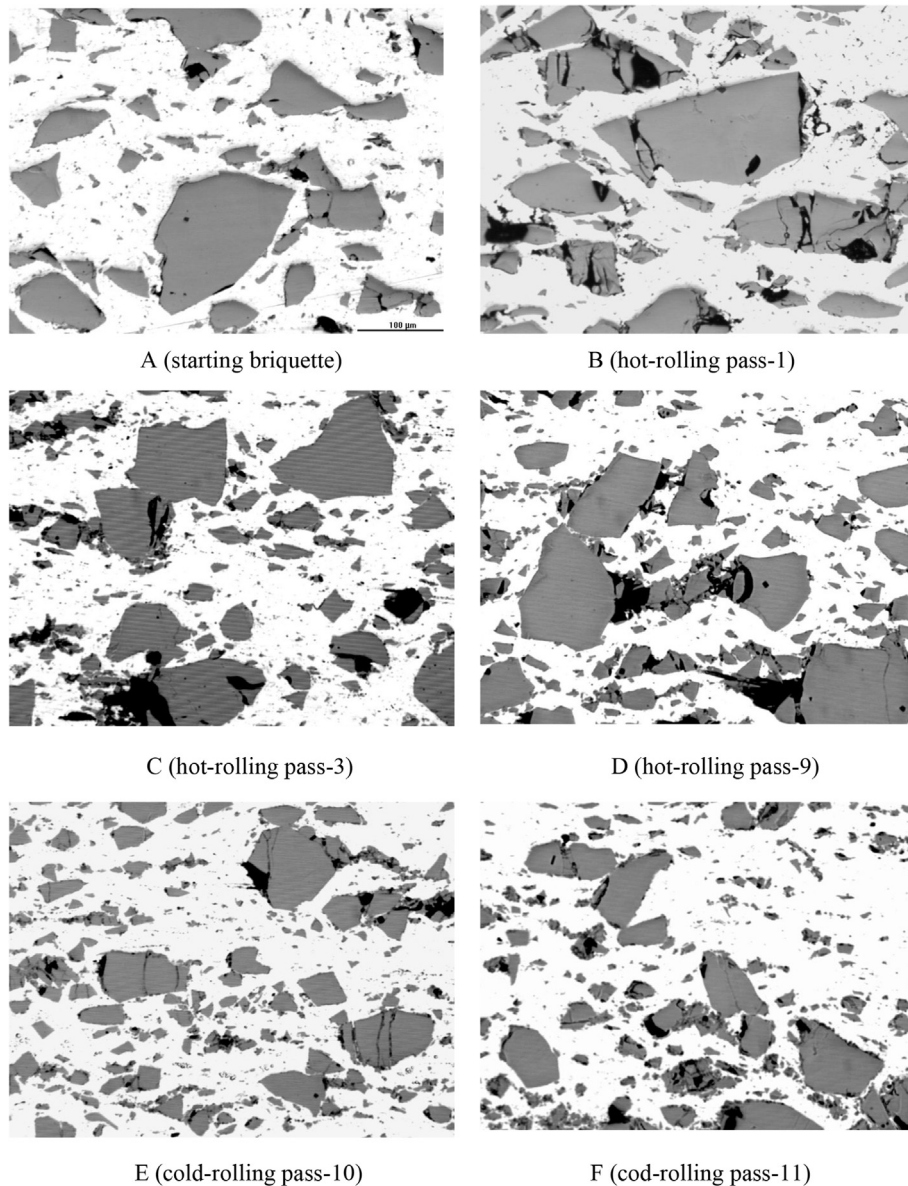


Fig. 15. Evolution of the meat microstructure during the rolling of a fuel plate.

U_3Si_2 particles with subsequent alignment of the fragments and formation of porosity in the rolling direction.

The residual porosity in the briquette is around 5 vol% and reaches around 6.5 vol% at the end of hot-rolling. In the cold-rolling, the residual porosity increases up to around 10 vol%. Because the assemblies are not bonded in the first four hot-rolling passes, the hydrostatic density determination (Archimedes Method) cannot be applied and therefore it is impossible to determine with accuracy the residual porosity in the fuel meat (the geometric method gives conflicting results).

By observing the micrographs of Fig. 7, voids arising from adjustments in the picture-frame assemblies are eliminated primarily in the first two hot-rolling passes. This illustrates why vent holes need to be left when welding cover plate to frame. After this initial elimination of the voids arising from mechanical adjustments, the void content reaches an equilibrium value that seems to be constant during all the hot-rolling steps. Probably this is due to an equilibrium reached between two opposite phenomena: pore formation due to fragmentation of U_3Si_2 particles and pore

elimination due to the aluminum matrix flow during hot-rolling. In the cold-rolling, the elimination of the pores formed due to fragmentation no longer occurs and the equilibrium is broken, which results in increasing residual porosity. These observations are in agreement with previous results reported in the literature [13].

For a more objective analysis of the U_3Si_2 particle fragmentation during rolling, the particle size distributions must be analyzed after each rolling pass. This was not done in this work.

Additional briquettes were fabricated with increasing residual porosities (up to 25 vol%). It was found that if the porosity of the briquette is higher than a critical value (approximately 15 vol% for the fuel with 3.0 gU/cm^3), it will crack during the first rolling pass. This demonstrates that the distribution of the powder into the die cavity should be very homogeneous when pressing the briquette. If a region of the die cavity contains a little quantity of powder, the residual porosity after pressing in this region will be very high, which inevitably will lead to the cracking of the fuel meat as can be seen in the radiograph shown in Fig. 16. At the beginning of the hot rolling, the briquette crack in regions of high porosity and the

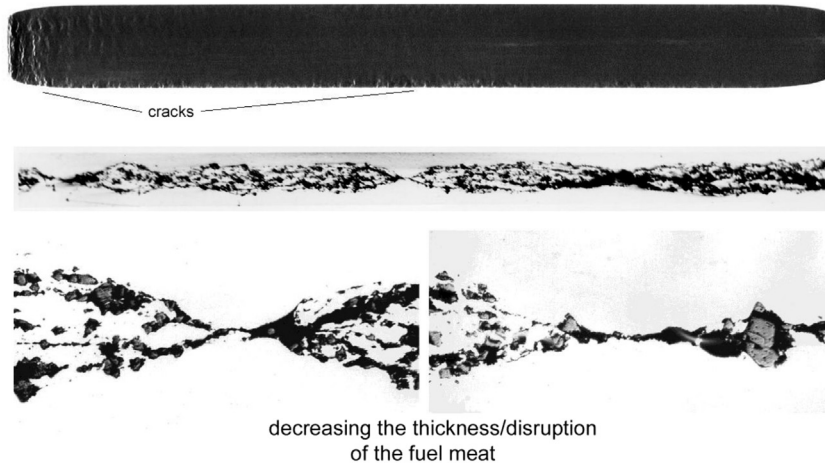


Fig. 16. Cracks in the fuel meat caused by poor distribution of powder into the die cavity during the pressing of the briquette (high voids content).

fragments move apart. During the hot-rolling, aluminum from the claddings fills the voids, resulting in the microstructure shown in the figure, where a region where the continuity of the meat is stopped can be observed.

3.5. Dimensional evolution with deformation

During the rolling operation, the fuel plate undergoes lengthening to a greater extent, as well as widening, which is small but not negligible. As the width and length of the meat of the finished fuel plate must meet specifications, the knowledge of these values due to the reduction in thickness of the assembly is an important tool, since it is data that may subsidize new designs or modifications of existing fuel designs. For a briquette rolled according to the rolling schedule presented in Tables 1 and 2, the total reduction is 83.5%. The lengthening factor (LF), which is defined as the length of the fuel meat for a given reduction in the rolling process divided by the initial length of the briquette (L_R/L_0), follows exponential law according to the following expression, which is valid for a uranium density of 3.0 gU/cm³, or 28 vol% U₃Si₂. Of course, the coefficients of the exponential equation will change for other uranium loadings. Fig. 17 summarizes the dependence of the lengthening factor on the accumulated reduction in thickness (AR) during rolling.

$$LF = 1.12 + 0.04 \cdot e^{AR/17.55} \tag{1}$$

where: LF = lengthening factor (L_R/L_0)

AR = accumulated reduction in thickness

The variation of the widening factor depending on the accumulated reduction in thickness during rolling is shown in Fig. 18. It is observed that in the first hot-rolling pass occurs an adjustment of the width of the briquette with the width of frame cavity. This should also occur in the case of the lengthening, but it is not noticeable in view of their high values compared with the values of widening. As the graph of Fig. 18 shows, in the first pass a large widening occurs (of about 2%), which is probably caused by an adjustment of the briquette to the frame. Another possible cause could be a misalignment of the assembly with the rolling cylinders at the entrance of the first pass, which may be caused by the small initial length of the assembly and by the irregular weld bead which hinders the use of the guiding devices. After this initial adjustment, the widening factor changes in a similar way to the lengthening

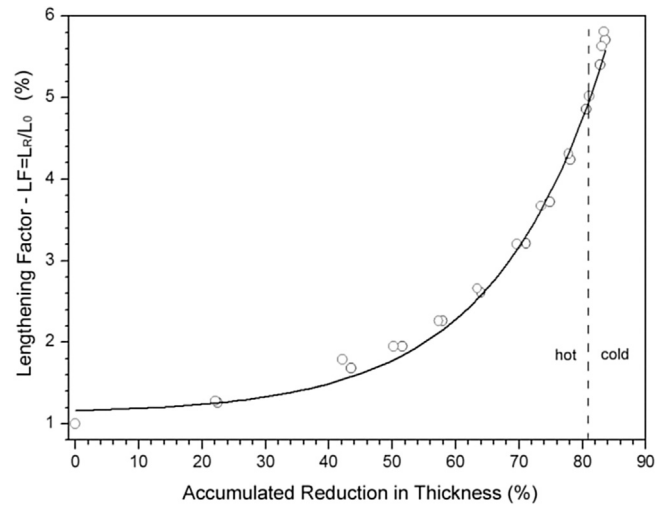


Fig. 17. Lengthening factor of the fuel meat according to the accumulated reduction in thickness during rolling.

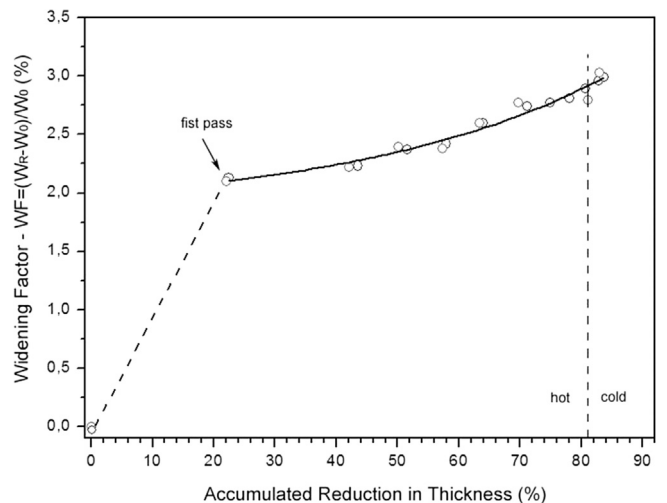


Fig. 18. Widening factor of the fuel meat according to the accumulated reduction in thickness during rolling.

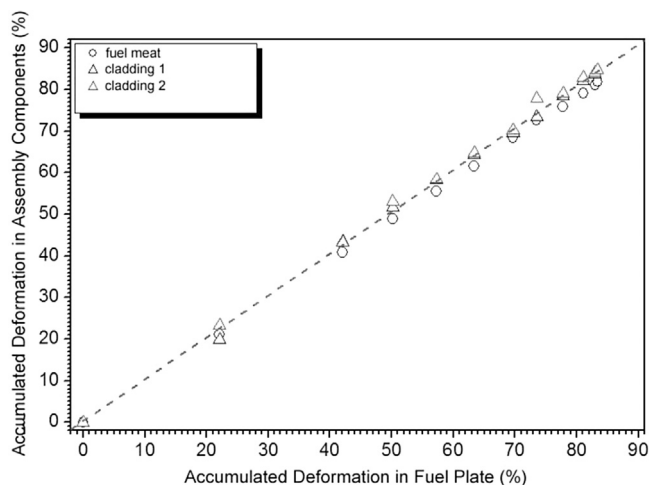


Fig. 19. Accumulated deformation of fuel meat and claddings compared to the accumulated deformation of fuel plate.

factor, varying exponentially with the accumulated reduction in thickness. The equation below presents the expression that represents the change of the widening factor (WF) according to the deformation in rolling. The widening factor is defined as the normalized difference between the width of the fuel meat for a given reduction in the rolling process and the initial width of the briquette $((W_R - W_0)/W_0)$.

$$WF = 1.84 + 0.05 \cdot e^{AR/41.47} \quad (2)$$

where: WF = widening factor $((W_R - W_0)/W_0)$

AR = accumulated reduction in thickness

The widening during rolling depends sensitively on the parallelism between the briquette and the lateral edge of the frame and cover plates. It also depends on the perpendicularity between the assembly and the rolls of the mill at the entrance of the pass. If the assembly does not enter perfectly perpendicular to the rollers, its widening will be greater the greater the deviation from perpendicularity. Because this feeding operation into rolls is manual, even with the aid of the roll-in table it is highly dependent on the operator. As lengthening depends on the widening, then lengthening also depends on the operator controlling the feeding operation into rolls since the core volume can be considered constant if

there is no significant variation in the porosity of the fuel meat during rolling.

The cladding and the meat thicknesses of the finished fuel plate are very important specifications for the fuel since the cladding ensures the insulation of the fuel meat from the reactor environment. If there is a cladding failure, the fuel meat is exposed and contamination with high activity radioactive material will occur. Depending on the design specification for the cladding and meat thicknesses for the fuel plate, the thicknesses of the initial cover plates and briquette must be precisely defined, which will define the final dimensions of the initial assembly to be rolled. This is a difficult task since the deformation of the meat and claddings are not equal to the total deformation experienced by the assembly, as illustrated in Fig. 19. This figure shows the relation between the reduction in fuel plate thickness (claddings plus meat) and the reduction effectively experienced by the individual components of the assembly, the meat and claddings. There is a tendency for the claddings to deform preferentially to the fuel meat. It is observed that the claddings undergo a greater deformation than the deformation of the fuel plate. Moreover, deformation of the fuel meat is smaller.

It is also noticed that the deformation experienced by each individual cladding is not exactly the same, which further complicates the design of the thicknesses of the initial picture-frame assembly. This also demonstrates the importance of ensuring the same surface quality of both rolls of the rolling mill and also the same lubrication condition.

The preferred deformation of the cladding is due to the higher resistance to deformation of the fuel meat caused by the presence of U_3Si_2 particles, which causes a greater lengthening in the claddings. As already discussed, this is the cause of the typical end defect known as “fish-tail”, illustrated in Figs. 3 and 7, which is caused by the difference in strength between the meat and the claddings. The fuel meat ends protrude into the frame/cladding interface by the forced deformation of the claddings, while the central meat region does not follow the deformation. The X-ray image presented in Fig. 20 shows a difference in the deformation of the claddings, where one end of the fish-tail is more elongated relative to the other (image was obtained after the eleventh rolling pass).

4. Conclusions

This study has extended the knowledge about the process of manufacturing fuel plates, showing the evolution of the main aspects of the fuel plate during deformation in rolling, such as defects,

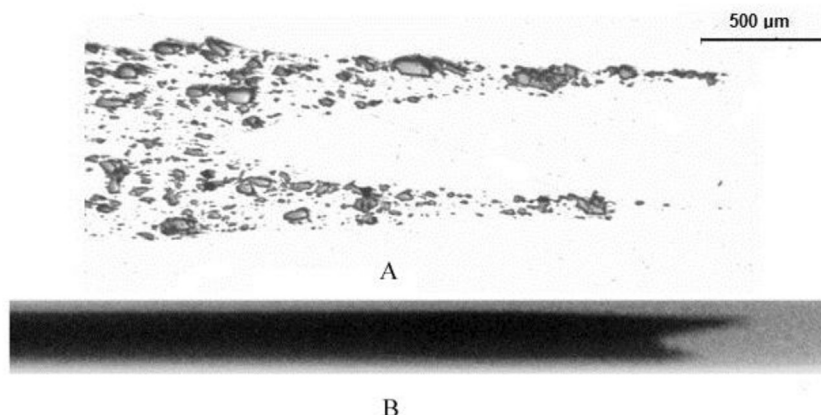


Fig. 20. Typical “fish-tail” end defect. A – optical micrograph, B – X-ray image.

fuel meat geometry and cladding and meat thicknesses.

The presence of structural defects such as cracks and fish tail in the fuel meats after rolling was studied. These defects were related to certain features of the assembly meat-frame-covers. It was found that the thickness of the briquette should be slightly greater than the frame thickness (0.1–0.2 mm) to minimize fish tail. The maximum acceptable gap between the briquette and the frame cavity to prevent cracks in the lateral of the fuel meat is around 0.2 mm, but interference fit is recommended.

Through an appropriate fuel plate rotation scheme for rolling, both main end defects (dog-boning and fish-tail) can be minimized and cambering can be controlled.

The uranium distribution homogeneity in the fuel meat is sensitive to the particle size distribution of the aluminum powder.

The fuel meat lengthening and widening were characterized for the specific rolling schedule and uranium density of the U_3Si_2 -Al fuel plate fabricated at IPEN. Both lengthening and widening varies exponentially with the accumulated deformation in rolling and depends sensitively on the practice of the operator in the feeding of the rolling mill rolls.

Most of the bonding between the components of the picture-frame assembly (meat-frame-claddings) continuously occurs up to the third hot-rolling pass. In the fourth pass it is still possible to observe small bonding imperfections and at the fifth pass the bonding is completed. The bonding begins at the center of the fuel plate and progresses in all directions to the extremities.

Fragmentation of U_3Si_2 particles was observed over all of the fuel meat deformation stages, the more markedly during cold-rolling. However, pronounced “stringering”, which is the alignment of the fragments in the rolling direction, was not observed.

Acknowledgments

The authors are grateful to CNPq for the research grants 304034/2015-0, 310274/2012-5 and 470363/2012-6 provided for this work.

References

- [1] A.R. Kaufman, *Nuclear Reactor Fuel Elements, Metallurgy and Fabrication*, Interscience, New York, N.Y., 1962.
- [2] J. E. Cunningham, E. J. Boyle, “MTR-Type fuel elements”. International Conference on Peaceful Uses of Atomic Energy. Geneva, 8–20 August, V. 9, pp. 203–7 (1955).
- [3] M. Durazzo, E. F. Urano de Carvalho, A. M. Saliba Silva, J. A. B. ASouza, H. G. Riella, “Current status of U_3Si_2 fuel elements fabrication in Brazil”. International Meeting on Reduced Enrichment for Research and Test Reactors – RERTR2007, Prague, 23–27 September, (2007). Washington: U.S. Department of Energy 2007. Available in: http://www.rertr.anl.gov/RERTR29/Abstracts/S11-8_Durazzo.html.
- [4] W.J. Kucera, C.F. Leitten, R.J. Beaver, Specifications and Procedures Used in Manufacturing U_3O_8 -aluminum Dispersion Fuel Elements for Core I of the Puerto Rico Research Reactor, Oak Ridge National Lab., Oak Ridge, Tn., 1963. ORNL-3458.
- [5] R.W. Knight, J. Binns, G.M. Adamson Jr., Fabrication Procedures for Manufacturing High Flux Isotope Reactor Fuel Elements, Oak Ridge National Lab., Oak Ridge, Tn., 1968. ORNL-4242.
- [6] R.J. Beaver, G.M. Adamson Jr., P. Patriarca, Procedures for Fabricating Aluminum-base ATR Fuel Elements, Oak Ridge National Lab, Oak Ridge, Tn., 1964. ORNL-3632.
- [7] J. A. Osso Jr, C.R.B.R. Dias, T. P. Brambilla, R. Teodoro, M. F. Catanoso, J. Zini, R.R.L. Bezerra, J. L. Vilella, J. L. Correia, E. Ivanov, F. M. S. Carvalho, L. Pozzo, P. L. Squair, J. Mengatti “Production of $99Mo$ at IPEN-CNEN/SP-Brazil”. In: 2013 Topical Meeting on Molybdenum-99 Technological Development, Chicago, Illinois, April 1–4, 2013.
- [8] J.A. Osso Jr., J.R. Teodoro, C.R.B.R. Dias, R.R.L. Bezerra, J.L. Vilella, J.L. Correia, J.A. Perrotta, G.A. Pereira, C.L. Zapparoli Jr., J. Mengatti, Brazilian Strategies to Overcome Molybdenum Crisis: Present and Future Perspectives of the Multipurpose Research Reactor, March 20–24, 2011, RRFM, Rome, Italy, 2011.
- [9] I.J. Obadia, J.A. Perrotta, A Sustainability Analysis of the Brazilian Multipurpose Reactor Project, March 21–25, 2010, RRFM, Marrakech, Morocco, 2010.
- [10] T. Goergeniy, U. Huth, Determination of cladding thickness in fuel plates for material test and research reactors (MTR), V. 4: Fuels (Appendices I–K), in: Research Reactor Core Conversion Guidebook, International Atomic Energy Agency, Vienna (Austria), April 1992, pp. 589–594, 594 pp..
- [11] International Atomic Energy Agency, Standardization of Specifications and Inspection Procedures for LEU Plate-type Research Reactor Fuels, International Atomic Energy Agency, Vienna, 1988. IAEA-TECDOC-467.
- [12] T. C. Weincek, “A study of the effect of fabrication variables on the quality of fuel plates”. In: RERTR INTERNATIONAL MEETING, November 3–6, 1986, Gatlinburg, Tenn, USA.
- [13] M. Martin, W.R. MARTIN, Fabrication Voids in Aluminum-base Fuel Dispersions, Oak Ridge National Lab, Oak Ridge, Tenn, October 1970. ORNL–4611.